 https://doi.org/10.1130/G45178.1

Long-term *in situ* observations on typhoon-triggered deep-sea turbidity currents

Yanwei Zhang[1*], Zhifei Liu[1], Yulong Zhao[1], Christophe Colin[2], Xiaodong Zhang[1], Meng Wang[1], Shaohua Zhao[1], and Benjamin Kneller[3]

[1] *State Key Laboratory of Marine Geology, Tongji University, Shanghai 200092, China*

[2] *UMR 8148 CNRS-GEOPS, Université de Paris-Sud, Orsay 91405, France*

[3] *School of Geosciences, University of Aberdeen, Aberdeen AB24 3UE, UK*

* Corresponding author. E-mail: ywzhang@tongji.edu.cn

This PDF file includes:

SUPPLEMENTARY MATERIALS AND METHODS

Measurements from the Subsea Mooring System

A deepwater subsea mooring system (TJ-G) was deployed at 2104 m water depth in the Gaoping Submarine Canyon (120.27°E, 21.66°N) for three and a half years from 25 May 2013 to 4 October 2016 (Fig. 1). The primary instruments on the mooring system include 2 sets of sediment traps (McLane MARK 78H-21), a 75 kHz long-ranger ADCP (TRDI Workhorse ADCP-LR75), a single-point recording current meter (Aanderaa Seaguard RCM) with temperature and turbidity probes, and a conductivity-temperature-depth (RBR-concerto CTD) with temperature and salinity sensors (Fig. 1C). The mooring system was usually retrieved in May, and redeployed following a quick maintenance at sea. An additional cruise was designed for monitoring the typhoon-triggered deep-sea turbidity currents with higher temporal resolution between 7 May and 4 October 2016.

Current velocities and echo intensity between 1664 m and 2048 m were recorded by the downward-looking ADCP every 1 hour from 25 May 2013 to 3 May 2016, and every 20 min from 7 May to 4 October 2016. Current velocities, temperature and turbidity at 2075 m were recorded by the RCM every 20 min from 25 May 2013 to 3 May 2016, and every 3 min from 7 May to 4 October 2016. Temperature and salinity at 2000 m were recorded by the CTD every 5 min from 11 May 2014 to 3 May 2016, and every 2 min from 7 May to 4 October 2016. All the data were averaged by 1 hour for consistency.

Settling suspended particles were collected with the cone-shaped time-series collecting sediment traps with 21 sampling bottles of 500 ml, filled with seawater containing $HgCl_2$ (3.3 g/l) and NaCl (35 g/l) to prevent microbial decomposition (Lahajnar et al., 2007). The traps have a sampling aperture of 0.05 m^2 covered with a polycarbonate hexagonal baffle. The sampling interval from 25 May 2013 to 3 May 2016 was 18 days, and from 7 May to 4 October 2016 was 7 days. The vertical sediment flux can be calculated by dividing the time interval of each bottle by the corresponding dried sample weight.

Tracking Typhoons across Taiwan

In order to assess the influence of typhoons over the northwest Pacific during the monitoring period, the metrics of tropical cyclones (such as their tracks, lifetime, and intensity) were analyzed with data from Unisys Weather (http://weather.unisys.com/ hurricane/). This dataset is based on Joint Typhoon Warning Center best track data, which provides the position and maximum sustained surface wind speed at 6-hour intervals. Here we only focus on strong tropical cyclones that satisfy the intensity criteria for typhoons (>33 m/s), which are linked to the turbidity currents in the Gaoping Submarine Canyon. Statistically, there were 16 typhoons that influenced this region between 1 May 2013 and 31 October 2016 (Fig. 1D).

Analysis of Meteorological and Hydrological Data for the Gaoping River

Atmospheric pressure from European Center for Medium-Range Weather Forecasts (ECMWF) and precipitation from the Tropical Rainfall Measuring Mission (TRMM), and river discharge as well as sediment content and load from Hydrological Year Book of Taiwan, are analyzed to identify the correlation between the atmospheric events and typhoon-triggered turbidity currents observed in the lower Gaoping Submarine Canyon. The data from ECMWF has a temporal resolution of 6 hours on a 0.125^{o} grid. The TRMM provides a daily temporal resolution on a 0.25^{o} grid. The Gaoping River daily discharge was recorded at the Liling Bridge gauging station, which is located at Zhongling Village, Dashu District, Kaohsiung City vicinity of the river upstream. The sediment content were also recorded at the Liling Bridge, but with tens of days' resolution omitting the transient maximal values. Atmospheric pressure and rainfall data are linearly interpolated into the location of Liling Bridge for better comparisons with local hydrological conditions of the Gaoping River. Precipitation data are available from https://disc2.gesdisc.eosdis.nasa.gov/, atmospheric pressure data were downloaded from https://www.ecmwf.int/, and discharge and sediment content for the Gaoping River can be downloaded from http://gweb.wra.gov.tw/.

Analysis of Earthquakes in the Southwestern Taiwan

Earthquake data from Central Weather Bureau (CWB) were analyzed in order to evaluate the role of earthquakes in triggering turbidity currents. Southwestern Taiwan within 150 km of the canyon head experienced 24 earthquakes of $M_L>4$ during the monitoring period. In February 2016, the Kaohsiung $M_L=6.5$ earthquake with a swarm of weaker after-shocks potentially associated with No. 19 turbidity current. There were no distinguishable turbidity currents consistently associated with other earthquakes. Earthquakes are therefore not the dominant trigger for these frequent turbidity currents observed in the deep submarine canyon.

Estimate of SSC from Turbidity

A proportional linear relation between the turbidity recorded by RCM and *in situ* SSC has been established in our previous studies (Zhang et al., 2014): SSC (mg/l) = 0.96 × turbidity (FTU). The same relation is adopted in this study.

Estimate of SSC from Echo Intensity

Echo intensity recorded by ADCP reflects the backscattering strength of the water, which is mainly due to the concentration of suspended particles and frequency of the acoustic signal. The volume backscattering strength *Sv* calibrated from the ADCP-recorded echo intensity has popularly been used to investigate sediment concentration and planktonic migrations (Gostiaux and van Haren, 2010; Zhao et al., 2015). The volume backscattering strength was calculated based on the following equation (Gostiaux and van Haren, 2010):

$$Sv = \left(10^{k_c E/10} - 10^{k_c E_r/10}\right) \times 10^{2\log_{10} R + 0.2\alpha R - A/10}$$

where *Sv* is the volume backscatter strength, E is the ADCP-observed echo intensity, E_r is the noise level of echo intensity, R is the distance along the acoustic beam, α is the attenuation coefficient of sound in sea water, k_c is the scale factor to convert echo intensity counts to decibels, and A is a constant. For TRDI Workhorse ADCP-LR75, E_r = 53 dB, α = 0.0245 dB/m, k_c = 0.5 dB/counts, and A = 105 dB are adopted.

The calibrated Sv nearest to the depth of RCM is then related to the SSC calculated from RCM-observed turbidity. It should be noted that the overlapped observation of echo intensity and turbidity only covers two periods, from May 2013 to January 2014 and from May to October in 2016, due to unexpected malfunction of instruments (Fig. DR3). As a result, a proportional relationship (SSC = 0.1Sv + 0.17, with R^2 = 0.97) between Sv and SSC has been established using the linear least-square fitting method with 95% confidence interval. Near-bottom SSC inferred from echo intensity and turbidity displays the same variability trend with reasonable discrepancies, especially during the strongest phase of turbidity currents in September 2016 (Fig. 3). This robust linearity is used to estimate empirically the profiles of SSC based on the ADCP-observed echo intensity, although potential uncertainties are unresolved.

Estimate of Sediment Transport

The near-bottom sediment transport was calculated with the following equation,

$$transport = \int_0^{z_h} SSC \cdot u \cdot L \cdot dz$$

where z_h is the thickness of high SSC exceeding 0.5 mg/l (as shown in Fig. 3D), u is the current velocity along canyon, L is the depth-averaged width of the canyon, calculated from the total cross-sectional area divided by depth (Fig. 1B). Besides, an approximate thickness z_h = 100 m is used when ADCP-based SSC is unavailable. It is noted that the sediment transport is underestimated due to the monitored slow-moving and more dilute part of the turbidity currents.

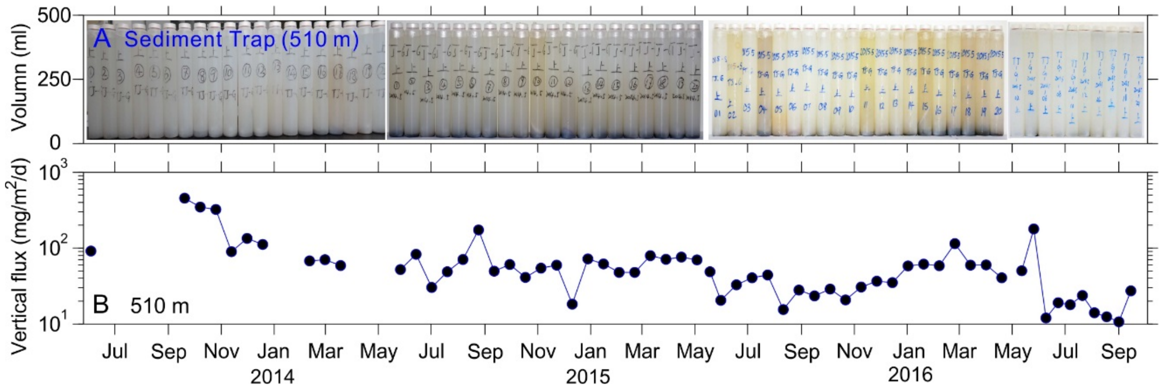

Figure DR1. A: Bottled sediment samples collected by the upper sediment trap at 510 m. **B**: The vertical sediment flux calculated from the dry weight of sediment trap samples shown in **A**.

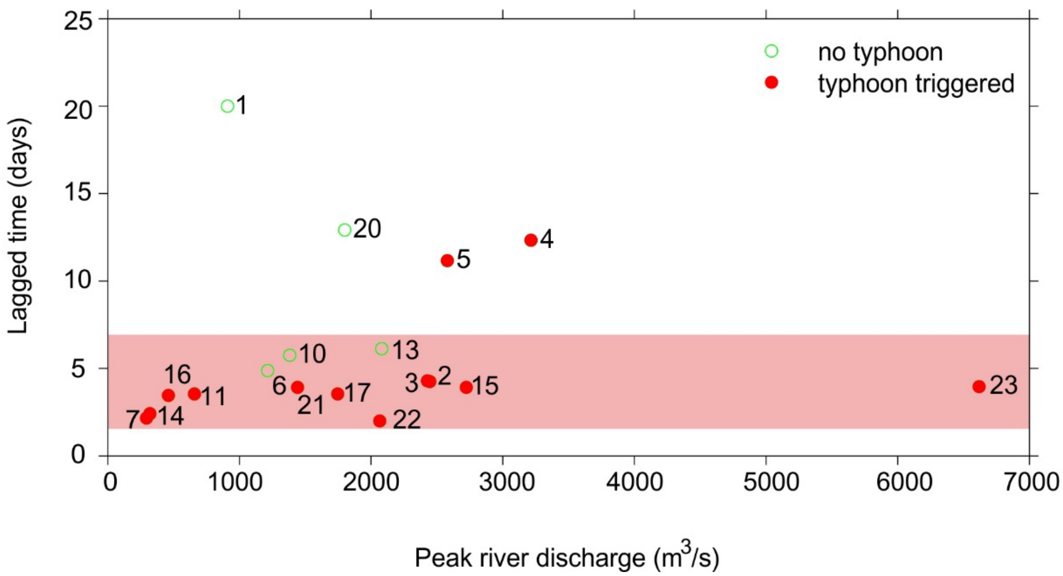

Figure DR2. Turbidity currents in the Gaoping Submarine Canyon lagging behind the peak river discharge at the canyon head. The lag time is the discrepancy between the peak river discharge at the canyon head and the peak of elevated SSC at TJ-G mooring site. A potential error of up to a day may exist since the river discharge is recorded as a daily average. Cases of both typhoon-related (red filled circles) and non-typhoon-induced (green open circles) river discharge are shown. The numbering of turbidity currents is as shown in Fig. 2E. The main lag time of between 2 and 7 days is shaded in light red.

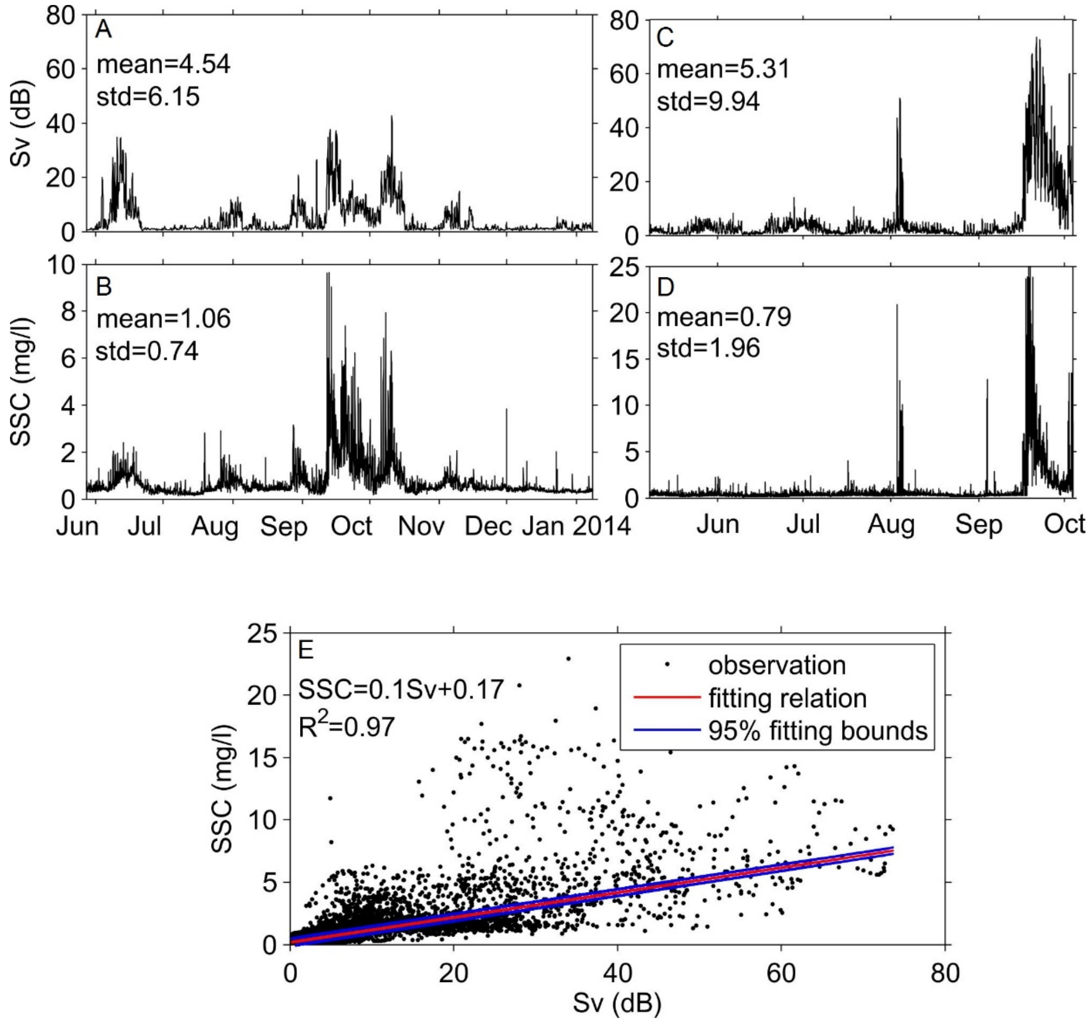

Figure DR3. Estimate SSC from volume backscattering strength *Sv* obtained by ADCP. **A**: Volume backscattering strength calibrated from the ADCP-recorded echo intensity between May 2013 and January 2014. **B**: SSC calibrated from RCM-recorded turbidity during the same period as in **A**. **C**: Same as in **A** but for the observation in 2016. **D**: Same as in **B** but for the observation in 2016. The corresponding mean value (mean) and standard deviation (std) of the data are labelled in each panel. **E**: Linear fitting between SSC and *Sv* shown in above panels in this figure. A proportional relationship (red line) is obtained with a high squared correlation coefficient (R^2=0.97). The 95% confidence interval is shown in blue lines.

TABLE DR1. TYPHOONS TRIGGERED DEEP-SEA TURBIDITY CURRENTS

No. of turbidity current	Arrival Time of turbidity current	End time of turbidity current	Duration of turbidity current (days)	Peak river discharge (m^3/s)	Lagged time (days)	Category and name of typhoon	No. of typhoon
1	2013/6/6 12:00	2013/6/22 9:00	15.90	909	20.0		
2	2013/7/17 18:00	2013/8/6 10:00	19.70	2447	4.3	4, Soulik	1
3	2013/8/26 19:00	2013/9/3 20:00	8.00	2428	4.3	1, Trami	2
4	2013/9/10 20:00	2013/10/3 11:00	22.60	3214	12.3	TS, Kong-rey	3
5	2013/10/3 16:00	2013/10/16 15:00	13.00	2579	11.2	5, Usagi	4
6	2014/5/26 9:00	2014/6/13 12:00	18.10	1215	4.9		
7	2014/6/14 16:00	2014/6/25 11:00	10.80	295	2.2	TS, Hagibis	5
8	2014/7/7 23:00	2014/7/9 14:00	1.60	/	/	4, Neoguri	6
9	2014/7/30 14:00	2014/8/17 18:00	18.20	/	/	2, Matmo	7
10	2014/8/19 6:00	2014/8/23 12:00	4.30	1383	5.8		
11	2014/9/25 1:00	2014/10/4 14:00	9.50	658	3.5	TS, Fung Wong	8
12	2015/2/17 16:00	2015/3/1 3:00	11.50				
13	2015/5/31 15:00	2015/6/28 5:00	27.60	2081	6.1		
14	2015/7/14 22:00	2015/7/30 11:00	15.50	320	2.4	4, Chan Hom	9
15	2015/8/12 10:00	2015/8/29 17:00	17.30	2724	3.9	5, Soudelor	10
16	2015/8/29 23:00	2015/9/28 9:00	29.40	461	3.5	4, Goni	11
17	2015/10/3 1:00	2015/10/12 1:00	9.00	1746	3.5	4, Du Juan	12
18	2016/1/12 18:00	2016/1/20 17:00	8.00				
19	2016/2/8 1:00	2016/3/19 21:00	40.80				
20	2016/6/26 10:00	2016/6/29 14:00	3.20	1800	12.9		
21	2016/7/14 10:00	2016/7/17 3:00	0.70	1442	3.9	5, Nepartak	13
22	2016/9/16 12:00	2016/10/2 11:00	16.00	2065	2.0	5, Mertanti/ 4, Malaksa	14/ 15
23	2016/10/2 11:00	/	/	6618	4.0	4, Megi	16

Note: Timing of turbidity currents is determined from the maximal value of SSC obtained at TJ-G mooring site, and peak river discharge is observed at the Gaoping River. The category of typhoons is based on wind speed (U, m/s) according to Saffir-Simpson scale. TS (Tropical storm): 17-33; Category 1: 33-43; Category 2: 43-50; Category 3: 50-59; Category 4: 59-69; Category 5: >69. The shaded cells show no significant river discharge or typhoons are observed. The cells with slashes indicate data are not available.

SUPPLEMENTARY REFERENCES CITED

Gostiaux, L., and van Haren, H., 2010, Extracting meaningful information from uncalibrated backscattered echo intensity data: Journal of Atmospheric and Oceanic Technology, v. 27, p. 943–949.

Lahajnar, N., Wiesner, M.G., and Gaye, B., 2007, Fluxes of amino acids and hexosamines to the deep South China Sea: Deep Sea Research Part I, v. 54, p. 2120–2144.

Zhang, Y., Liu, Z., Zhao, Y., Wang, W., Li, J., and Xu, J., 2014, Mesoscale eddies transport deep-sea sediments: Scientific Reports, v. 4, doi: 10.1038/srep05937.

Zhao, Y., Liu, Z., Zhang, Y., Li, J., Wang, M., Wang, W., and Xu, J., 2015, In situ observation of contour currents in the northern South China Sea: Applications for deepwater sediment transport: Earth and Planetary Science Letters, v. 430, p. 477–485.